MINIATURE ELECTRODE ARRAY AND SYSTEM FOR EXPERIMENTAL SURFACE EEG RECORDINGS

B. AMUZESCU[*#], *G. COCINĂ*[**], *Ş. FLORICĂ*[***]

[*]Deptartment of Biophysics & Physiology, Faculty of Biology, University of Bucharest
91–95, Splaiul Independenței, București 050095, Romania,
[#]E-mail: bogdan@biologie.kappa.ro
[**]Smart Systems Consulting SRL, P.O. Box 2-263, Bucharest 014730 Romania,
E-mail: smartsysconsult@gmail.com
[***]Deptartment of Geology, Faculty of Biology & Geology, "Babeş-Bolyai" University,
1 M. Kogălniceanu Street, Cluj 400294 Romania,
E-mail: stefan_stefan2121@yahoo.com

Abstract. We describe design, construction, testing, and use of an advanced electroencephalography (EEG) system for experimental surface recordings on small laboratory animals. Signals are collected with a miniature electrode array containing 8 longitudinal bipolar leads and a ground electrode, preamplified 2000-fold with headstage miniature circuits based on low-offset zero-drift op-amps in an instrumentation amplifier design, then filtered via 6th order Chebyshev active filters with passing band 0–35 Hz, sampled at 1 kHz and recorded with standard electrophysiology equipment. We determined the transfer functions (gain and phase shift) for different preamplifier circuits and the filters. A real-life test of the equipment was performed on an adult male Wistar rat weighing 310 g following headstage placement under diethylether anesthesia. The recording had a typical shape; its Fourier transform indicated higher spectral power density in the δ and θ range of frequencies (1–7 Hz), as well as β rhythm.

Key words: EEG, zero-drift operational amplifier, instrumentation amplifier, Chebyshev active filters, signal ground, chassis ground, transfer function, multi-electrode array.

INTRODUCTION

Experimental recording of brain electrical activity represents a long-lasting field of research shaped by a number of landmark achievements. Following experimental proof of brain biopotentials and currents, of positive potential of cortical surface at rest and negative shifts during activity obtained *via*

Received December 2016;
in final form January 2017.

ROMANIAN J. BIOPHYS., Vol. 26, No. 2, P. 69–82, BUCHAREST, 2016

galvanometric measurements by Richard Caton and communicated in 1875, and direct recordings of brain electrical activity in experimental animals with a mirror galvanometer on photographic paper obtained by Pravdich-Nieminski in 1912, the intense pioneering research of Hans Berger during the years 1924–1929 settled the field of clinical electroencephalography (EEG) [5]. It is worth noting that the interest of Berger in this method stemmed from his desire to provide a scientific explanation for telepathy, awaken by a strange personal experience. In early studies Berger described the basic rhythm at rest in vigil state recorded in occipital leads with closed eyes, in the 8–12 Hz frequency range, known as α rhythm spindles or Berger waves, as well as their cessation and replacement by faster β rhythms (13–35 Hz) at eye opening. Regarded with suspicion and distrust by fellow clinicians at the beginning, Berger's findings were confirmed during the 1930s by British electrophysiologists Edgar Douglas Adrian and B.H.C. Matthews. The clinical use of electroencephalography was broadened and consolidated by systematic studies performed during the 1930s–1940s by Harvard researchers Frederic and Erna Gibbs (authors of a famous and very comprehensive clinical EEG atlas), joined by Hallowell Davis and William Lennox, particularly in the field of epilepsy [5].

Despite its tremendous success in clinical research and current medical practice, surface EEG has been used on a much narrower scale as an experimental neurophysiology research method applied to small laboratory animals, being largely replaced by field potential recordings with stereotaxically implanted electrodes and arrays, *in vivo* patch-clamp and imaging, and *in vitro* studies on brain slices or dissociated primary neuronal-glial preparations. In recent years a number of research instrumentation companies offered equipments for *in vivo* electrophysiology recordings on small laboratory animals, with real-time data transmission on multiple channels using wired or wireless systems. These include Triangle Biosystems International (the implantable wireless systems of the IW series or surface headstage systems of the W series with simultaneous transmission on 5 to 126 channels with a minimum sampling rate of 50 kHz / channel: http://www.trianglebiosystems.com/products.html) that can be used with the silicon microelectrode arrays produced by Cambridge Neurotech (http://www.cambridgeneurotech.com/), or the wireless data acquisition and transmission systems produced by MultiChannel Systems, with parallel wireless data transmission on 4, 8, 16 or 32 channels, or stationary systems with 64 to 256 channels, allowing simultaneous electrical or optical stimulation (http://www.multichannelsystems.com/products/vivo-me-systems). However, all these systems were specifically devised for use with stereotaxically implanted electrodes or microelectrode arrays (MEA), *i.e.* via an invasive technique. Therefore, we aimed to develop a system for noninvasive EEG recordings in small laboratory animals using surface electrodes, with 8 channels in parallel. We have chosen signal transmission via shielded cables between preamplifiers located in a

headstage unit and the final stages connected to a standard electrophysiology data acquisition interface (Digidata 1440A) driven by the pClamp10 software.

MATERIALS AND METHODS

In building the amplifier we attempted to reproduce the technical specifications of EEG amplifiers of the Biopac system (model EEG100C, Biopac Systems Inc., Goleta, CA): gain 50000 ×, passing band 0–35 Hz limited by active filters. We took special precautions for design and construction of electronic circuitry to limit noise and electrical interference: preamplifier modules placed in a headstage unit, with a high common mode rejection rate (CMRR), coupled to the electrodes via short connections within the shielded metal case of the headstage, use of a signal ground electrically separated from the chassis ground, coupled to a grounding electrode placed on the midline in an anterior position, transmission of signals of all 8 channels via shielded wires, including the signal ground and positive and negative power supply (with shields connected to the chassis ground), electrical supply of preamplifiers and filters from pairs of batteries located in the shielded case of the main unit, effective low-pass filtering of amplified signals *via* analog active filters with very steep transfer function, providing a passing band up to 35 Hz and marked dampening (~0.01) at 50 Hz, the frequency of the alternative current supply network, placement of experimental animals subjected to EEG recording in a Faraday cage.

ELECTRODE PLACEMENT AND LEADS DIAGRAM

We have chosen a leads diagram with 8 bipolar leads (Fig. 1) inspired from the 10–20 EEG electrode system proposed in 1949 by H.H. Jasper for human surface EEG recordings [2] and a longitudinal bipolar leads diagram [4]. Electrode placement took into account the skull size, shape, anatomy, and position of the brain of an adult male Wistar rat weighing 290 g [6]. The miniature electrode array covers an area on 9 mm in length located on the skull between bregma and lambda. The posterior electrodes are placed on the binaural line, corresponding to the transversal position of the lambdoid fissure. Distances between electrodes are 5 mm in the longitudinal direction and slightly shorter in the transversal direction. The electrodes were made of silver wire of electrolytic purity and 0.25 mm in diameter (AGW1030, World Precision Instruments, Sarasota, FL) by local melting of an end upon brief insertion in the flame of a gas burner to obtain small pearls approximately spherical in shape. The electrodes were inserted in small predrilled orifices obtained by punching with dissection microtweezers an elastic double membrane cut from a laboratory glove (Nitrilex PF, Mercator Medical, PL), sticked

with cyanoacrylate glue and soldered to the corresponding wires of the preamplifier signal entries. Thereafter the membrane with electrodes was glued to the bent long edges of the inferior side of the metal box of the headstage, with dimensions of 23×13×16 mm. This headstage, containing the preamplifiers, is placed on the head of a rat during a brief anesthesia with diethylether after shaving the appropriate area of the skull, and fixed with silk adhesive tape for medical use, before placing the animal in the recording cage. The membrane with the electrode array has to be carefully positioned, symmetrical relative to the longitudinal median line, with the posterior electrodes along the transversal binaural line, at the level of external auditory orifices. All experimental procedures for recordings in animals were in agreement with EC Directive 2010/63/EU, observed the 3R principles (reduce, refine, replace), and were approved by the institutional ethics committee.

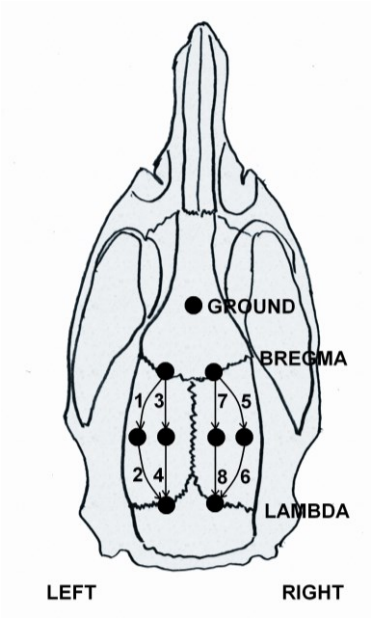

Fig. 1. Wiring diagram for the 8 longitudinal bipolar leads and the ground electrode, with placement of electrode array on an adult rat skull.

ELECTRONIC DESIGN OF HEADSTAGE PREAMPLIFIERS

The preamplifiers of the EEG system have to fulfill a series of requirements, including a very high input impedance, a large passing band, reduced drift and voltage offset, a high common mode rejection rate, reduced internal noise, distortions and nonlinearities of the transfer function, a steady phase shift in the

passing band, stable functioning, resistance to perturbations and external electrical shocks, reduced electrical energy consumption.

We tested successively different circuitry designs based on integrated differential operational amplifiers with field effect transistors (FET) in the input stage. The first tested circuit (Fig. 2a) contained two amplifying stages with negative resistive feedback (one of the simplest constructive variants), using two operational amplifiers of the LF347N integrated circuit [7], a low-cost high-speed quad op-amp with JFETs in the input, with an internally adjusted voltage offset, produced using the BI-FET II™ technology. The typical input voltage offset of this circuit amounts to 5 mV, the input current offset to 25 pA, the input bias current to 50 pA, and the input resistance to 10^{12} Ω at 25 °C. The circuit was powered by a pair of 9 V batteries, and was tested by applying at the input a sinusoidal signal provided by a sine wave generator with adjustable frequency, with a peak-to-peak amplitude of 20 mV, after passage through a resistive potentiometric divider of 1 MΩ /1 KΩ, resulting in a peak-to-peak entry signal level of 20 μV, typical for a surface EEG signal. The output signal of the sine wave generator and the output signal of the tested preamplifier were displayed on the two channels of a digital oscilloscope (model TDS210, Tektronix, Beaverton, OR). The gains of the two stages of the amplifier, set by the ratios of feedback and input resistors, were 100× and 500×, resulting in a total gain of 50000×, typical for an EEG amplifier. The test revealed a large input voltage offset, that could be corrected by applying a direct current offset correction *via* a multiturn potentiometer connected to the power supply pair of batteries and coupled *via* a resistor to the circuit input in a summation configuration, and, even more annoying, an important drift resulting in rapid entry of the amplifier in a saturation regime.

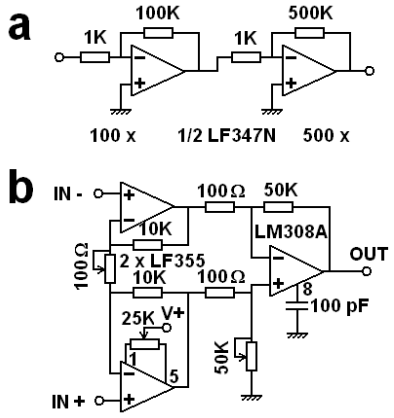

Fig. 2. Two preamplifiers tested in preliminary experiments. a. Two-stage resistive feedback differential amplifier; b. instrumentation amplifier with high input resistance and reduced drift.

To correct these deficiencies, we built a differential amplifier based on the principle of instrumentation amplifiers (Fig. 2b), using two LF355 op-amps [8] for the inverting and non-inverting input of the common stage, represented by a LM308A bipolar transistor op-amp featuring low voltage offset and drift [9]. Beyond high input impedance, instrumentation amplifiers (INA) offer the advantage of a high common mode rejection rate, and convenient adjustment of gain by the ratio between the equal resistances of the feedback loops of the two entry op-amps (R_F) and the R_G resistance that connects these two stages (name derived from *R* gain – the resistance that sets the gain, usually an external resistor for integrated INA circuits) [10]. A large variety of integrated INAs are presented in a Texas Instruments application note: Instrumentation Amplifiers – they're not op amps but what are they? [11]. The gain of the differential entry stage is $G = 1 + 2\ R_F/R_G$, and the supplementary CMRR has the same value, because the common mode potential passes this stage unamplified, with gain $G = 1$ [3]. In addition, the model that we tested offers the choice of manual input voltage offset compensation via an adjustable multiturn potentiometer of 25 kΩ connected to pins 1 and 5 of the op-amp of the (+) input and to the positive power supply. By testing this circuit in conditions similar to the previous one, we noticed improved performance, due to the option of manual voltage offset correction, but drift remained a significant problem. The circuit remained stable for a limited time and featured a continuous drift of the output signal until saturation was reached.

To solve this difficult problem, important for biopotential amplifiers, we used a modern integrated op-amp (launched in November 2015 by Texas Instruments), very effective in terms of voltage offset and drift: TLV4333 [12] (in the microencapsulated surface-mounted device – SMD – variant TSSOP-14, with external dimensions 5.00 × 4.40 mm). This circuit is a high-performance low-cost CMOS operational amplifier that employs a proprietary self-calibration technique, providing a low voltage offset (maximally 15 μV) and an almost zero time and temperature drift at a maximal idle current of 28 μA. The input and output are rail-to-rail, and the $1/f$ noise is almost flat, rendering it an ideal circuit in a variety of applications, particularly biomedical applications. In addition, the circuit is optimized for low voltage power supply, in the range from ±0.9 V to ±2.75 V, or between 1.8 V and 5.5 V with unique source; therefore it can be connected to a pair of 1.5 V AAA size batteries or accumulators. Internal offset corrections are performed at 8 μs intervals, using a proprietary technique involving digital sampling, unaffected by aliasing errors or flickering noise up to 125 kHz. The incorporated low-pass filter features a cut-off frequency of approximately 8 MHz

(at –3 dB) and a roll-off slope of 20 dB/decade, reducing the susceptibility to electromagnetic interference by shifts due to signal rectification in the internal semiconductor junctions of the circuit.

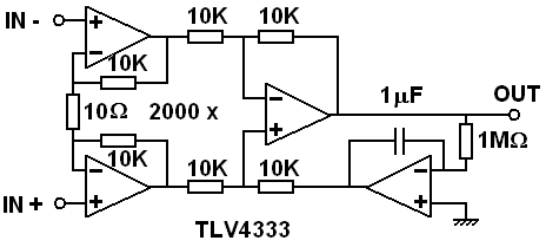

Fig. 3. INA preamplifier with reduced voltage offset and drift, based on quadruple operational amplifier TLV4333.

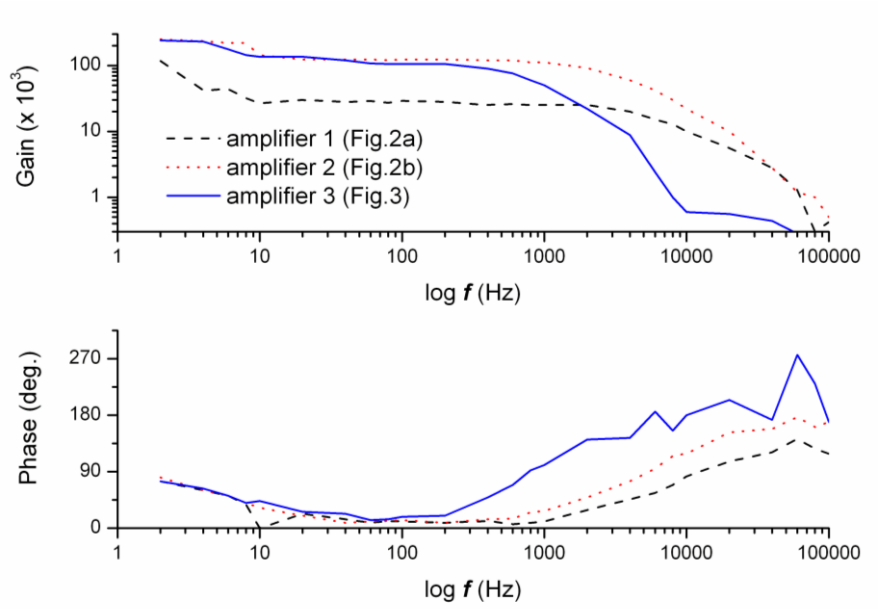

Fig. 4. Transfer functions (gain and phase shift) for the three tested preamplifier circuits.

The circuit that we built and tested (Fig. 3) represents an instrumentation amplifier featuring a 2000× gain (2000× in the first differential stage and 1× in the common stage, thus providing a good common mode rejection), coupled to an activated RC high-pass filter placed in a feedback loop, with the output applied to

the non-inverting input of the common stage, following a construction proposed by Thomas Kugelstadt in the previously cited article [3]. The printed circuit boards (PCB) were designed using specific software and produced with a milling machine with numeric control. The PCB surface is 20×9.5 mm, allowing placement of preamplifiers for four channels on the two sides of a double-plated PCB (two channels on each side, built around TLV4333 quadruple amplifiers). The resistors and capacitors were of miniature size (SMD varieties), placed in the immediate neighborhood of the integrated circuits pins, thus minimizing electrical interference and capacitive or inductive couplings, and the special design of the printed circuits also contributed to reduced electromagnetic coupling and interference.

The functional tests performed with the sine wave generator in similar conditions with those used for previous circuits confirmed the proper functioning of all eight channel preamplifiers. The transfer functions of the three tested circuit variants were obtained with the sine wave generator and digital oscilloscope in the frequency range 2–100 000 Hz (Fig. 4).

ACTIVE LOW-PASS FILTERS FOR THE BAND 0–35 HERTZ

The passing band of these preamplifiers is quite large (on the order of tens of kHz), therefore the radiofrequency noise and internal noise of these stages have to be eliminated by filtering, given that the useful EEG signal is confined to the band 0–35 Hz. Therefore, we used a series of cascade active filters of voltage-controlled voltage source (VCVS) type, in the variant of Sallen-Key filters. These filters comprise a succession of two passive RC filters in the input, but the passive component, that should have been connected to the ground of the first passive RC pair, is instead connected in a feedback loop to the operational amplifier output, resulting in a transfer function with pronounced slope, due to reduction in attenuation at lower frequencies via this feedback, thus producing a "knee" in the frequency response function, and a higher slope of this transfer function compared to a purely passive RC filter. By different placement of R and C elements one can obtain different variants: low-pass, high-pass, or band-pass. By multiplying the number of stages, the transfer function becomes even steeper. By varying the values of RC elements and amplifying factors (via adjustment of resistors in the negative feedback loop) one can obtain transfer functions reproducing those of various types of passive analog filters: Butterworth, Bessel, Chebyshev, etc. We have chosen a 6^{th} order Chebyshev filter because it offers the steepest transfer function for the same order of the filter, with the disadvantage of ondulations or ripple in the passing band. This is a minor disadvantage, because we have chosen a reduced ripple level (0.5 dB), and the slope of the transfer function is steep enough to provide a dampening of the order of 1% at 50 Hz, the frequency of the alternative current power supply network, for a passing band of 35 Hz. The

constructive secret that ensures the success of such a block of filters consists in a perfect match of R and C values of each RC group according to the formula $RC = 1 / 2\pi c_n f_c$, with f_c = 35 Hz and different c_n coefficients for each stage. The values and circuit diagram were applied from the textbook of Horowitz & Hill [1].

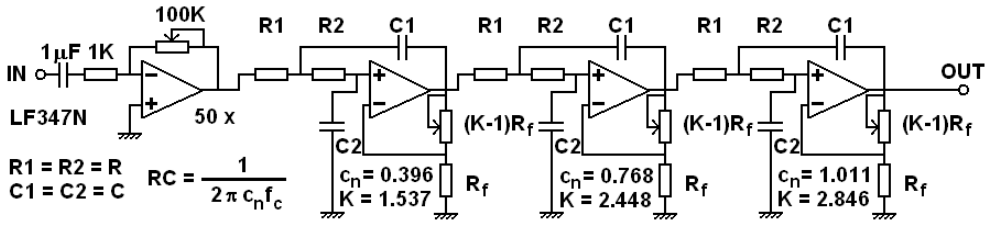

Fig. 5. Assembly of inverting operational amplifier (used to adjust total gain of EEG channel) and block of 6th order Chebyshev active filters built around an LF347N quadruple op-amp.

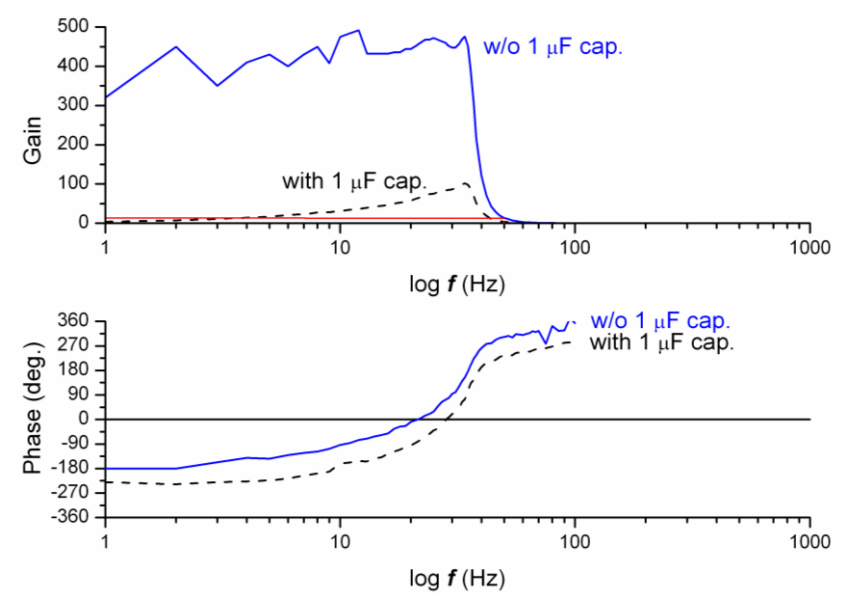

Fig. 6. Transfer function of the assembly of channel amplifier 6th order Chebyshev low-pass active filter block (gain and phase shift) with and without 1 μF passage capacitor at the input.

We used polystyrene capacitors of 100 nF (nominal value); all capacitors were measured with a precision capacity meter and paired such that the two capacitors of each stage did not differ by more than 0.25 nF. The resistances of each RC pair were precisely computed and were obtained by fine adjustment of

precision multiturn potentiometers during continuous measurement with a digital ohmmeter. The transfer functions of the blocks of 6th order Chebyshev active filters were satisfying, in agreement with those published in Horowitz & Hill [1]. The operational amplifiers used for the filter blocks were LF347N (quadruple op-amps); for each LF347N integrated circuit, three of the amplifiers were used for the three consecutive stages of the filter, while the fourth amplifier for an inverting amplifier stage with resistive feedback, with a gain of ~50×, adjusted via a multiturn potentiometer placed in the feedback loop, having a non-polarized 1 µF passage capacitor at the input, and the total gain of the preamplifier-amplifier-filter block assembly was set to 50000× (Fig. 5).

In addition, the printed circuit containing the assemblies of amplifiers-filter blocks includes a circuit for decoupling the signal ground from the chassis ground, achieved with a LF355 op-amp in a voltage follower circuit (impedance adaptor), to avoid injection of chassis ground noise (acquired, for example, *via* connection with the digitizer) into the signal ground. For the same purpose, the shields of connection wires from the headstage to the main unit, connected to the chassis ground, are completely decoupled from the signal ground or from the metal case of the headstage.

After achievement of the filters, we studied the transfer function of the amplifier-filter block assembly for an EEG channel (Fig. 6). The gain and phase shift (in degrees) were measured by applying a sine wave signal at the input, having fixed amplitude (20 mV or 100 mV peak-to-peak) and variable frequency in the range 1–100 Hz, produced by the sine wave generator used in previous tests, and by measuring the input and output signals with the Tektronix TDS210 digital oscilloscope, using the MEASURE, CURSORS and RUN/STOP functions of this instrument. The presence of the 1 µF passage capacitor at the input introduces an important frequency-dependent dampening, therefore we decided to exclude this capacitor from the circuit.

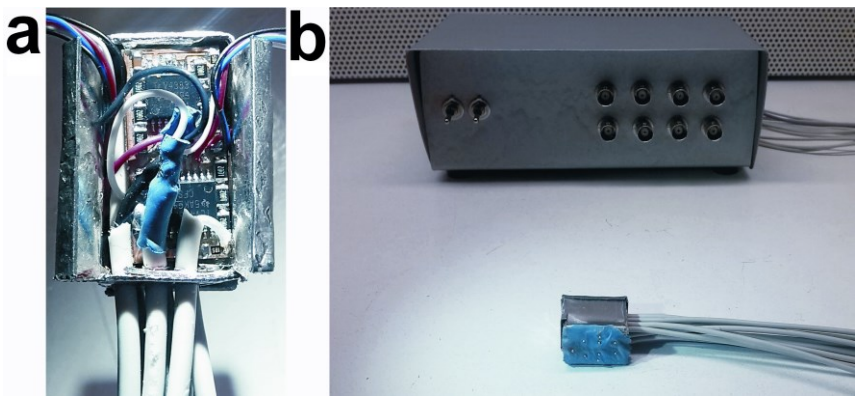

Fig. 7. Headstage and main unit of EEG system. a. Detailed view of the headstage before attachment of electrode array; b. Overall image of central unit and headstage, connected by the bundle of shielded wires.

RESULTS AND DISCUSSION

ASSEMBLY AND TESTING OF THE EEG EQUIPMENT

In Fig. 7 we present images of the headstage and of the main unit of the EEG equipment, containing the blocks of amplifiers-filters, the two pairs of batteries (of 9 V and 1.5 V), and the outputs connected to BNC sockets of the 8 channels, and in Fig. 8 a brief stretch of EEG recording performed on a male Wistar rat weighing 310 g in a right fronto-parietal lead and its Fourier transform, featuring increased spectral power density in the δ and θ range, as well as in the β range, corresponding to the vigil state of the recorded subject.

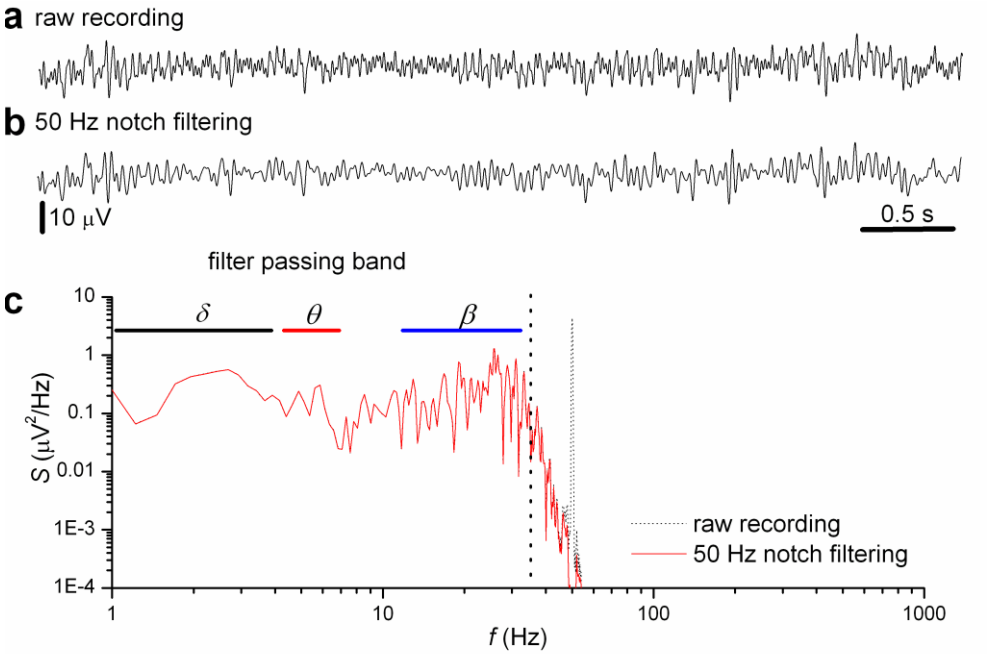

Fig. 8. A 5-s stretch of EEG recording in right fronto-parietal lead in an adult male Wistar rat and its Fourier transform, a. raw recording; b. after applying the 50 Hz notch filter of pClamp10 (identical time and amplitude scales in a. and b.); c. Fourier transform of raw and filtered signal and power spectrum showing peaks in the δ–θ and β bands.

The performance of our EEG equipment was fairly good and similar to that of commercial systems for monitoring brain electrical activity in freely moving small laboratory animals, like those presented within the introduction, although we have to emphasize that, upon our knowledge, this is the only system and electrode

array specifically designed and built for surface EEG recordings on small animals. All other commercial systems are designed for implanted electrodes or arrays of electrodes. We want to emphasize particularly the low noise of the output signal, resulting from a combination of factors including presence of a headstage preamplifier, good shielding and grounding, separation of signal ground from chassis ground, and the performance of analog active filters. The residual noise can be further eliminated via digital filtering (*e.g*. using the 50 Hz notch filter implemented in Clampfit10).

CONCLUSION

In conclusion we have developed and tested a reliable 8-channel EEG system suitable for surface recordings in small laboratory animals, with an electrode array adapted for the skull and brain size and anatomy of adult rats. The system can be used in a wide variety of experimental settings for neurophysiology applications, animal models of disease (focal ischemic stroke, induced epileptogenic foci by stereotaxic injection of picrotoxin or kainate, etc.), as well as for pharmacology and experimental therapy studies.

Acknowledgements. The authors gratefully acknowledge Prof. Valeriu Neştianu and Dan Psatta for instructive discussions, Dr. Emanuel Drăgan for experimental support. The study was funded from partnership grant PN2 80/2012 to Prof. Aurel Popa-Wagner.

REFERENCES

1. HOROWITZ, P., W. HILL, *The Art of Electronics*, 3rd edition, Cambridge Univ. Press, Cambridge MA, 2015, pp. 242, pp. 407–409.
2. KLEM, G.H., H.O. LÜDERS, H.H. JASPER, C. ELGER, The ten-twenty electrode system of the International Federation, in Recommendations for the Practice of Clinical Neurophysiology: Guidelines of the International Federation of Clinical Physiology (EEG Suppl. 52) G. Deuschl, A. Eisen eds., Elsevier Science B.V., 1999, pp. 3–6.
3. KUGELSTADT, T., Getting the most out of your instrumentation amplifier design, *Analog Applications Journal*, 2005, **4Q 2005**, 25–29.
4. NEŞTIANU, V., D. CIOROIANU, F. ROMANESCU, A. NEŞTIANU, N. RUŞCĂ, R. HUREZEANU, D. GEORGESCU, Noţiuni de tehnică a înregistrării şi prelucrării EEG. EEG patologică – Epilepsia – MEG, in *Neuroelectrofiziologie clinică*, L. Zăgrean ed., Ed. Medicală, Bucureşti, 2005, pp. 332–368.
5. NIŢĂ, D.A., Ritmuri cerebrale în somn şi în veghe, in *Neuroelectrofiziologie clinică*, L. Zăgrean ed., Ed. Medicală, Bucureşti, 2005, pp. 298–329.
6. PAXINOS, G., C. WATSON, *The Rat Brain in Stereotaxic Coordinates*, 5th edition, Elsevier Academic Press, Burlington MA, 2005.
7. * * *, *LF147/LF347 Wide Bandwidth Quad JFET Input Operational Amplifiers*, Texas Instruments application note SNOSBH1D – MAY 1999 – REVISED MARCH 2013, pp. 1–21.

8. * * *, *LF155/LF156/LF256/LF257/LF355/LF356/LF357 JFET Input Operational Amplifiers*, National Semiconductor application note DS005646, December 2001, pp. 1–23.
9. * * *, *LM108A/LM208A/LM308A Operational Amplifiers*, National Semiconductor application note TL/H/7759 (Texas Instruments SNOSBS6A), May 1989, pp. 1–9.
10. * * *, *Best of Baker's Best – Amplifiers*, Texas Instruments application note slyc124, 2016, pp. 1–28.
11. * * *, *Instrumentation Amplifiers – they're not op amps but what are they?*, Texas Instruments application note, 2016, http://e2e.ti.com/support/amplifiers/precision_amplifiers/w/design_notes/1777.
12. * * *, TLVx333 2-μV VOS, 0.02-μV/°C, 17-μA, CMOS Operational Amplifiers Zero-Drift Series, Texas Instruments application note SBOS751, December 2015, pp. 1–34.